Journal of Inflammation Research

Dovepress
Taylor & Francis Group

Open Access Full Text Article

ORIGINAL RESEARCH

SPP1 as a Prognostic and Immunotherapeutic Biomarker in Gliomas and Other Cancer Types: A Pan-Cancer Study

Kan Wang[1,*], Jinxin Wan[2,*], Ruipeng Zheng[1,*], Yifei Xiao[1], Fengjun Lv[1], Haitao Ge[1], Guang Yang[3], Yu Cheng[1]

[1]Department of Neurosurgery, The First Affiliated Hospital of Harbin Medical University, Harbin City, Heilongjiang Province, 150007, People's Republic of China; [2]Department of Neurosurgery, Guangdong Provincial People's Hospital, Zhuhai Hospital (Jinwan Central Hospital of Zhuhai), Zhuhai City, Guangdong Province, 519090, People's Republic of China; [3]Department of Neurosurgery, The Second Affiliated Hospital of Fujian Medical University, Quanzhou, Fujian Province, 362000, People's Republic of China

*These authors contributed equally to this work

Correspondence: Yu Cheng, Department of Neurosurgery, The First Affiliated Hospital of Harbin Medical University, Harbin City, Heilongjiang Province, 150007, People's Republic of China, Email ccyy30@126.com; Guang Yang, Department of Neurosurgery, The Second Affiliated Hospital of Fujian Medical University, Quanzhou, Fujian Province, 362000, People's Republic of China, Email 151534363@qq.com

Background: Gliomas, including glioblastoma (GBM), present significant treatment challenges due to their poor prognosis and complex tumor microenvironment. This study investigates the role of Secreted Phosphoprotein 1 (SPP1) as a prognostic and immunotherapeutic biomarker in gliomas and other cancers through pan-cancer analysis.

Methods: A comprehensive pan-cancer analysis was conducted using datasets from UCSC TCGA Pan-Cancer, TCGA-GBM, UALCAN, and single-cell sequencing data from GEO and TISCH. The correlation of SPP1 expression with overall survival (OS), progression-free survival (PFS), immune cell infiltration, and immune checkpoint markers was analyzed. Functional validation was performed via SPP1 knockdown in glioma cell lines to evaluate effects on proliferation, invasion, and immune interactions.

Results: SPP1 was found to be overexpressed in 27 tumor types, with high expression correlating with poor OS, PFS, and increased immune cell infiltration, particularly with CD8+ T cells and macrophages. Single-cell analysis indicated SPP1 enrichment in macrophages interacting with malignant GBM cells. Knockdown of SPP1 significantly inhibited glioma cell proliferation, invasion, and promoted apoptosis.

Conclusion: The findings suggest that SPP1 is a promising target for immunotherapy, potentially improving outcomes for patients with gliomas and other cancers. Further research is warranted to explore SPP1-targeted therapies and their efficacy in clinical settings.

Keywords: SPP1, glioblastoma, immunotherapy, biomarker, prognosis

Introduction

Cancer remains one of the leading causes of death worldwide. Despite significant advances in treatment methods, the prognosis for many cancer types remains poor. Therefore, identifying new biomarkers and therapeutic targets is crucial for improving the survival rates and quality of life for cancer patients.[1] Gliomas, a class of highly invasive brain tumors, pose significant treatment challenges and have poor prognoses. Despite employing multiple treatment modalities such as surgery, radiotherapy, and chemotherapy, the five-year survival rate for glioma patients remains below 10%.[2]

In recent years, immunotherapy has emerged as a promising treatment strategy, demonstrating substantial potential in various cancers.[3] Novel immunotherapeutic approaches, including immune checkpoint inhibitors, CAR-T cell therapy, and cancer vaccines, have achieved remarkable success in certain solid tumors.[4] However, their efficacy in gliomas has been limited, potentially due to the complex tumor microenvironment and immune evasion mechanisms. Thus, exploring new immunotherapeutic targets and strategies is imperative.

Received: 7 November 2024
Accepted: 5 February 2025
Published: 13 February 2025

SPP1, also known as osteopontin, is a phosphorylated glycoprotein widely expressed in various tissues and cells. *SPP1* plays critical roles in cell adhesion, migration, survival, and immune regulation.[5] Previous studies have demonstrated that *SPP1* is aberrantly overexpressed in various cancers and is closely associated with tumor aggressiveness and patient prognosis. Specifically, *SPP1* has shown potential as a prognostic marker in breast cancer, lung cancer, colorectal cancer, and other solid tumors.[6] Additionally, *SPP1*'s role in the tumor microenvironment has garnered significant attention, as it is involved in immune cell infiltration, cytokine secretion, and immune evasion mechanisms.[5,7]

However, the expression characteristics of *SPP1* in gliomas and its potential as a prognostic and immunotherapeutic biomarker across multiple cancer types remain to be fully elucidated.[8] This study aims to investigate the potential value of *SPP1* as a prognostic and immunotherapeutic biomarker in various cancer types, including gliomas, through pan-cancer analysis. We will systematically analyze *SPP1* expression levels and their association with patient prognosis and immunotherapeutic responses, aiming to reveal the potential of *SPP1* as a novel immunotherapeutic target. We hope this research will provide new insights and directions for cancer diagnosis and treatment, thereby improving clinical outcomes for patients.

Material and Methods

Data Collection

The comprehensive analysis in this study utilized pan-cancer data sourced from the UCSC TCGA Pan-Cancer database (https://xenabrowser.net/). This dataset was employed for investigations into gene expression, prognostic assessments, and immune analyses. Moreover, the Cancer Genome Atlas TCGA-GBM dataset, specifically obtained from the TCGA database, was utilized for analyzing gene expression and clinicopathological features. The UALCAN database, which is derived from the Clinical Proteomic Tumor Analysis Consortium (CPTAC) and the International Cancer Proteogenome Consortium, offers data on 13 tumor types, such as colorectal cancer, breast cancer, ovarian cancer, clear cell renal cell carcinoma, uterine corpus endometrial carcinoma, gastric cancer, glioblastoma, pediatric brain tumors, head and neck squamous cell carcinoma, lung adenocarcinoma, lung squamous cell carcinoma, liver cancer, pancreatic cancer, and prostate cancer. Through the "Pan-cancer View" module, we could visualize the protein expression profiles of 10 types of tumors and their corresponding adjacent tissues. By selecting the "CPTAC" module and entering the target gene SPP1, followed by choosing the "Pan-cancer View" module, we observed the protein expression of SPP1 in cancerous and adjacent tissues across various tumor types.

Prognostic Analysis

We employed the Gene Expression Profiling Interactive Analysis 2 (GEPIA2) platform (http://gepia2.cancer-pku.cn/) to conduct Kaplan-Meier survival analysis. Utilizing the "Survival Analysis" module, we generated Kaplan-Meier (K-M) plots to examine OS and DFS associated with SPP1 across multiple cancer types. Subsequently, the "Expression DIY" module was used to illustrate the correlation between SPP1 expression levels and cancer staging in various malignancies.

To delve deeper into the relationship between gene expression and patient prognosis, we accessed data on DSS and PFS from the TCGA patients, available via the Xena database. Survival analysis for each cancer type, considering a significance level of $P<0.05$, was performed using the Kaplan-Meier method, analyzed with the "survival" and "survminer" R packages. Furthermore, Cox proportional hazards analysis was carried out using the "survival" and "forestplot" packages to investigate the association between gene expression and survival outcomes.

Immune Correlation and Gene Mutation Analysis

We utilized the SangerBox platform to investigate the relationship between SPP1 expression and ESTIMATE scores, as well as tumor-infiltrating immune cells (TIICs) across various cancers. This analysis included CD4+ T cells, CD8+ T cells, B cells, neutrophils, macrophages, among others. Additionally, we examined the association between SPP1 expression and immune cells using various tools such as MCPcounter, XCELL, IPS, CIBERSORT, the expanded multidimensional immune characterization (EPIC), and tumor immune dysfunction and exclusion (TIDE) across a pan-cancer cohort.

We employed the R package "ESTIMATE" to analyze the correlation between SPP1 expression and ESTIMATE scores specifically in GBM patients. Further, through the SangerBox platform, we explored the relationship between SPP1 expression and immune checkpoints (ICP) in various tumors within the TCGA cohort. The immune checkpoint genes analyzed included HAVCR2, CD276, IL10, TGFB1, VEGFA, IL4, TNFSF4, CD28, ICOS, ENTPD1, ICAM1, TNFRSF9, and CD80. Spearman rank correlation tests were performed to determine partial correlations and associated p-values.

We also investigated the correlation between SPP1 expression levels and immune cell infiltration in LGG and GBM. Additionally, mutation data specific to gliomas were obtained from the TCGA. To assess mutation frequencies, patients were divided into two groups based on SPP1 expression levels: the lowest 25% and the highest 25%, using the R package "maftools".

Correlation Analysis Between SPP1 and Microsatellite Instability

The uniformly standardized pan-cancer dataset was sourced from the UCSC database (https://xenabrowser.net/), specifically the TCGA Pan-Cancer (PANCAN) dataset, which comprises 10,535 samples and 60,499 genes. From this dataset, we extracted expression data for the SPP1 gene, focusing on samples categorized as Primary Blood Derived Cancer - Peripheral Blood and Primary Tumor. The Microsatellite Instability (MSI) scores for each tumor type were obtained from an earlier study.[9] We combined the MSI scores with the gene expression data, applying a log2(x+0.001) transformation to normalize each expression value. Cancer types with fewer than three samples were excluded from the analysis, resulting in a dataset that includes expression data for 37 cancer types.

Gene Expression and Enrichment Analysis

A protein-protein interaction network was constructed using data from the STRING database (https://cn.string-db.org/cgi/about). Through the "Correlation Analysis" module of GEPIA2 (http://gepia2.cancer-pku.cn/), we identified the top 100 genes showing significant correlation with SPP1 across pan-cancer datasets. The top 30 genes, selected based on p-value rankings, were visualized using Cytoscape.

Gene Ontology (GO) analysis, encompassing biological processes, molecular functions, and cellular components, is widely used for comprehensive functional enrichment studies. The Kyoto Encyclopedia of Genes and Genomes (KEGG) provides a recognized repository for information on genomes, biological pathways, diseases, and drugs. We performed GO annotation analysis and KEGG pathway enrichment analysis on the differentially expressed genes, employing the clusterProfiler R package. A false discovery rate (FDR) threshold of < 0.05 was applied to determine statistical significance.

Correlation Between SPP1 Expression and Pathways

This study used previously collected gene sets related to various pathways.[10] The analysis was conducted using the "ssgsea" parameter in the GSVA R package. According to the ssGSEA algorithm, the enrichment score for each pathway in each sample was calculated sequentially, resulting in the connection between samples and pathways. By calculating the correlation between gene expression and pathway scores, we could determine the relationship between SPP1 and the relevant pathways.

Single-Cell Sequencing Data Analysis

The scRNA-seq data for GBM tissues were obtained from the GEO scRNA-seq dataset (GSE131928) and the Glioma_GSE131928_10X dataset, which is available in the Tumor Immune Single Cell Hub (TISCH) database (http://tisch.comp-genomics.org/home/).[11] The single-cell expression matrix was normalized using the NormalizeData method in the "Seurat" package, with the raw counts (UMI) scaled to 10,000 counts per cell. Quality control, clustering, and cell type annotation were performed using the uniform analysis algorithm (MAESTRO). The GSE131928 dataset includes a total of 13,553 cells derived from 9 GBM tissues.

Drug Sensitivity Analysis

We conducted chemotherapy drug sensitivity and immunotherapy response predictions. To assess susceptibility between high TCR risk groups and low TCR risk groups, we employed the pRRophetic R package, constructing ridge regression models with 10-fold cross-validation to estimate IC50 values. Data on various common antitumor drugs, including CUDC-101, GSK690693, Imatinib, LAQ824, and OSI-027, along with their genomic profiles, were sourced from the largest public pharmacogenomics database, the Cancer Drug Sensitivity Genomics (GDSC) (https://www.cancerrxgene.org/).

Analysis of RNA Modification Genes

We downloaded the pan-cancer dataset, TCGA TARGET GTEx (PANCAN, N=19131, G=60499), from the UCSC database (https://xenabrowser.net/), which has been standardized. From this dataset, we extracted the expression data for the marker gene SPP1 and 44 genes associated with three types of RNA modifications (m1A (10), m5C (13), m6A (21)) across all samples. We specifically filtered samples sourced from Primary Solid Tumor, Primary Tumor, Primary Blood Derived Cancer - Bone Marrow, and Primary Blood Derived Cancer - Peripheral Blood, excluding all normal samples. Each expression value was then transformed using log2(x+0.001). Following this, we calculated the Pearson correlation between SPP1 and marker genes associated with five immune pathways.

Analysis of SPP1 and Tumor Stemness

We downloaded the uniformly standardized pan-cancer dataset from the UCSC database (https://xenabrowser.net/). From this dataset, we extracted the expression data for the SPP1 gene in each sample. The samples were then screened, and the RNAss tumor stemness score for each tumor, calculated based on mRNA features, was obtained from prior research [9]. The stemness indices and gene expression data were integrated, and each expression value was further transformed using a log2(x+0.001) transformation. Cancer types with fewer than three samples were excluded, resulting in expression data for 37 cancer types. As depicted in the figure, significant correlations were observed in 20 tumors, with 1 tumor exhibiting a significant positive correlation and 19 tumors showing significant negative correlations.

Cell Culture and Transfection

U251, LN229, U87, A172, T98G, and NHA cells were provided by Procell Life Science & Technology (Wuhan, China) and cultured at 37°C in DMEM (Seven, Beijing, China) supplemented with 10% FBS (Invitrogen, USA) and 5% CO2. For the experimental study, cells in the logarithmic growth phase were selected. SPP1-siRNA was obtained from Genechem (Shanghai, China). For transfection using SPP1-siRNA and Lipo3000 (Solarbio, Beijing, China), cells were cultured to the logarithmic growth phase and adjusted to a density of 70–90%. SPP1-siRNA was mixed with Lipo3000 in Opti-MEM medium at a ratio of 1:1 to 3:1 to form complexes. The complexes were added to the cell culture plate, gently swirled to mix, and incubated for 4–6 hours. Subsequently, the medium was replaced with fresh medium containing 10% FBS, and the cells were cultured for an additional 48–72 hours for further analysis.

qRT-PCR Analysis

First, extract total RNA from cells or tissues and treat with DNase I to remove genomic DNA contamination. Then, use reverse transcriptase to convert the RNA into cDNA. Prepare the qRT-PCR reaction mix, including the cDNA template, specific primers, SYBR Green dye, and qPCR buffer. Load the reaction mix into a qPCR machine and set appropriate thermal cycling conditions for amplification. Monitor the accumulation of fluorescence signal from SYBR Green to detect the amplification products. Finally, quantify the target gene expression levels using a standard curve or the ΔΔCt method.

Western Blot Analysis

First, extract proteins from cells or tissues and quantify them using a BCA assay kit. Separate the protein samples by SDS-PAGE electrophoresis, then transfer the proteins onto a PVDF membrane. Block the membrane with 5% milk or BSA, then incubate with the primary antibody overnight. After that, incubate with the secondary antibody for 1 hour. Finally, visualize the protein bands using ECL detection reagent.

Cell Viability Analysis

Cells were plated in 96-well plates at a density of $2x10^3$ cells per well, using DMEM as the culture medium. After undergoing various treatments, the cells were cultured for 24 and 48 hours. Subsequently, 10 μL of CCK8 reagent was added to each well, and the plates were incubated at 37°C for 1 hour. The absorbance at 450 nm was then measured for each well using a microplate reader.

Colony Formation Assay

Cells (500 cells/well) were seeded in 6-well plates and cultured for 10–14 days. After washing with PBS, cells were fixed with 4% paraformaldehyde for 15 minutes and stained with 0.5% crystal violet for 30 minutes. Colonies with more than 50 cells were counted under a microscope. Each experiment was performed in triplicate.

Invasion Assay

For the invasion assay, chamber inserts were coated with 40 μL of BD Matrigel (Corning, USA) and allowed to solidify at 37°C for 1 hour. Approximately 50,000 cells, suspended in 500 μL of DMEM without FBS, were added to the upper chamber of the insert. The insert was then placed in a 24-well plate containing 750 μL of DMEM supplemented with FBS. After a 24-hour incubation period, the cells that had invaded through the insert were fixed with 4% paraformaldehyde, stained with 0.05% crystal violet, and quantified under a microscope.

Cancer Cell Spheroid Invasive Assay

U251 and LN229 cell spheroids (500 cells per drop) were generated using the hanging drop method on the lids of culture dishes. After 48 hours, the spheroids were collected, mixed with rat tail type I collagen, and embedded into wells to create a 3D culture system. Invasion was assessed 3 days later by measuring the maximum invasive distance and invaded area using ImageJ.

Flow Cytometric Analysis

After harvesting the cells, they were washed with pre-cooled PBS and then resuspended in pre-cooled 70% ethanol, followed by fixation at 4°C for 24 hours. The cells were then washed with PBS, and propidium iodide reagent (Beyotime, Shanghai, China) was added. The samples were incubated at 37°C for 30 minutes in the dark. Red fluorescence was detected at an excitation wavelength of 488 nm using flow cytometry, alongside light scattering detection. DNA cell cycle analysis was performed using FlowJo software to quantify the cell cycle distribution.

Cells were seeded in 6-well plates and treated according to experimental conditions. After 48 hours, cells were collected, washed twice with cold PBS, and resuspended in 100 μL of binding buffer. Annexin V-FITC (5 μL) and propidium iodide (PI, 5 μL) were added to the suspension and gently mixed. The mixture was incubated in the dark at room temperature for 15 minutes. After incubation, 400 μL of binding buffer was added, and samples were analyzed using flow cytometry within 1 hour to quantify the percentage of apoptotic cells. Each experiment was performed in triplicate.

Statistical Analysis

All data calculations and statistical analyses were conducted using R software (https://www.r-project.org/, version 4.0.2). For comparisons of continuous variables between two groups, an independent Student's *t*-test was utilized to assess the statistical significance of normally distributed variables. For non-normally distributed variables, the Mann–Whitney *U*-test was employed. Statistical p-values were two-tailed, with a significance threshold set at $P<0.05$.

Results

Overexpression of SPP1 in Various Cancer Types

The expression of SPP1 in 33 types of human cancers was analyzed using the TCGA and GTEx datasets. The results showed that this gene was significantly overexpressed in 27 tumor tissues, including GBM, LGG, ACC, BLCA, CHOL, COAD, ESCA, UCEC, UCS, BRCA, CESC, LUAD, LUSC, LIHC, HNSC, DLBC, TCGT, THCA, PAAD, PRAD,

PCPG, STAD, SKCM, OV, READ, STES, and KIRC. However, its expression was downregulated in tumor tissues such as KIRC, KICH, and SARC (Figure 1A–C). At the protein level, we evaluated the expression of SPP1 using the Clinical Proteomic Tumor Analysis Consortium database. Our analysis showed elevated levels of SPP1 in all cancer types studied, including head and neck squamous cell carcinoma (HNSC), pancreatic cancer (PAAD), uterine corpus endometrial carcinoma (UCEC), glioblastoma, liver cancer, and lung cancer, compared to normal tissues (Figure 1D). We further investigated the relationship between SPP1 expression and tumor grade using the online database Sangerbox (http://sangerbox.com/home.html). The analysis results indicated a consistent correlation between elevated SPP1 expression and higher tumor grades in HNSC, LIHC, GBM, LGG, and PAAD (Figure S1A). In MESO and TGCT, SPP1 expression was associated with tumor M stage (Figure S1B). In LUAD, COAD, READ, PRAD, HNSC, LIHC, PAAD, TGCT, and BLCA, SPP1 expression was significantly correlated with tumor N stage (Figure S1D). For tumor T stage, SPP1 expression was significantly correlated with COAD, READ, BRCA, ESCA, STES, KIRP, KIRC, STAD, PRAD, HNSC, LIHC, and BLCA (Figure S1C). In COAD, READ, HNSC, ESCA, STES, KIRP, STAD, PRAD, KIRC, LIHC, and BLCA, SPP1 expression was significantly correlated with tumor staging (Figure S1E).

Correlation Between SPP1 Expression and Tumor Prognosis

Our analysis results showed that SPP1 expression is significantly correlated with clinical staging and grading in various tumors. This finding prompted us to further investigate the prognostic impact of SPP1 expression in these specific cancers. The study's analysis results demonstrated significant statistical differences in OS data across multiple tumors with SPP1 expression, including glioblastoma (GBM, P=8.1e-42, HR: 1.63 [1.52, 1.76]), lower-grade glioma (LGG, P=3.6e-11, HR 1.47 [1.31, 1.64]), liver hepatocellular carcinoma (LIHC, P=3.1e-6, HR 1.13 [1.07, 1.19]), pancreatic cancer (PAAD, P=3.3e-3, HR 1.19 [1.06, 1.33]), and head and neck squamous cell carcinoma (HNSC, P=0.03, HR 1.06 [1.01, 1.12]). This finding suggests that SPP1 expression profoundly impacts the survival time of patients with these cancer types. Progression-free survival (PFS) data indicate that SPP1 plays a crucial role in GBM (P=3.2e-35, HR: 1.50 [1.40, 1.60]), LGG (P=7.4e-10, HR: 1.34 [1.22, 1.47]), and LIHC (P=1.4e-3, HR: 1.07 [1.03, 1.11]). Notably, elevated SPP1 expression is positively correlated with GBM and LGG. Moreover, disease-free survival (DFS) analysis shows that SPP1 expression is significant in ESCA (P=1.6e-3, HR 1.32 [1.10, 1.57]) and PAAD (P=4.2e-3, HR 1.40 [1.10, 1.79]). Regarding disease-specific survival (DSS), our analysis indicates that SPP1 has an adverse impact on GBM (P=5.0e-39, HR 1.65 [1.53, 1.78]), LGG (P=3.4e-11, HR 1.50 [1.33, 1.69]), and PRAD (P=2.9e-3, HR 1.22 [1.07, 1.39]). These findings collectively suggest that SPP1 significantly affects various survival parameters, including OS, PFS, DFS, and DSS, for GBM (Figure S2A–D). Additionally, KM-plot survival analysis indicates that high SPP1 expression is associated with poor OS in six types of cancers, including ACC, CESC, HNSC, LGG, LIHC, and LUAD (Figure 2A and B). SPP1 expression is closely related to DFS in LGG and ESCA patients (Figure 2C and D). These findings underscore the critical importance of further exploring the role of SPP1 in gliomas due to its considerable clinical and scientific significance.

Relationship Between SPP1 Expression and Tumor Immunity

We employed multiple methods, including EPIC, MCPcounter, XCELL, QUANTISEQ, TIMER, and CIBERSORT, to predict immune infiltration and investigate the association between abnormal SPP1 expression and stromal cells in the tumor microenvironment across various cancers. The results showed significant correlations across all six methods, indicating that SPP1 is significantly associated with B cells and macrophages in several cancer types, including GBM. In the TIMER analysis, SPP1 expression exhibited significant positive correlations with CD4+ cells and macrophages in GBM, COAD, LGG, LIHC, OV, PRAD, and THCA (Figure 3A–F). Further correlation analyses using different tumor immune infiltration methods revealed that SPP1 expression is significantly associated with various immune cells, immune-related genes, and immune checkpoint-related genes across multiple tumor types (Figure 3G and H). Additionally, we examined the correlation between SPP1 expression and immune microenvironment scores in glioma patients, finding a positive correlation between SPP1 expression and immune scores (Figure 3I and J). These findings suggest that SPP1 expression may be closely linked to immune cell infiltration in gliomas and the immune response in diverse tumor microenvironments.

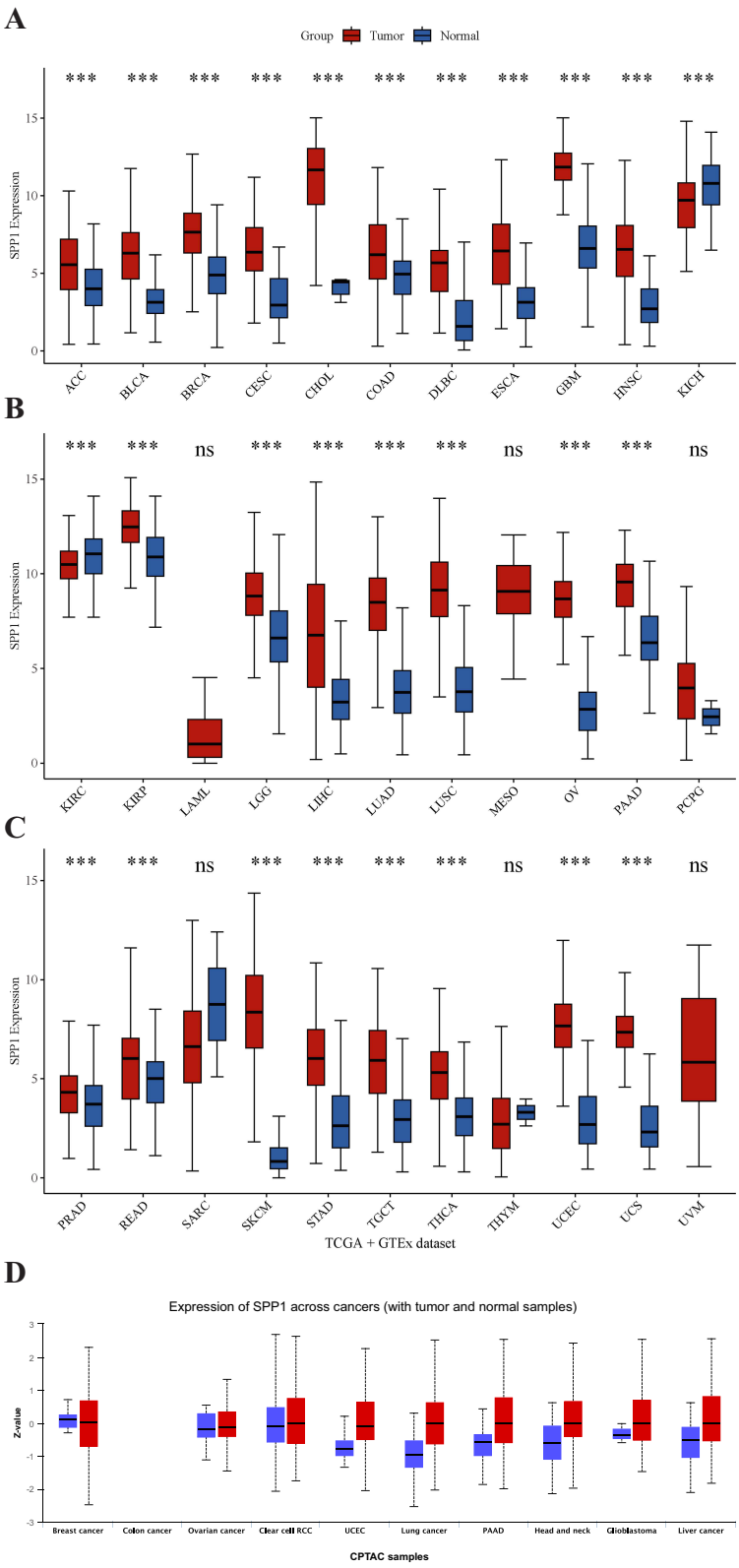

Figure 1 Analysis of *SPP1* Expression in 33 Cancer Types. (**A**–**C**) Analysis of *SPP1* expression in 33 cancer types using TCGA and GTEx databases. ***p < 0.001. (**D**) CPTCA analysis of *SPP1* expression in cancer.

https://doi.org/10.2147/JIR.S505237

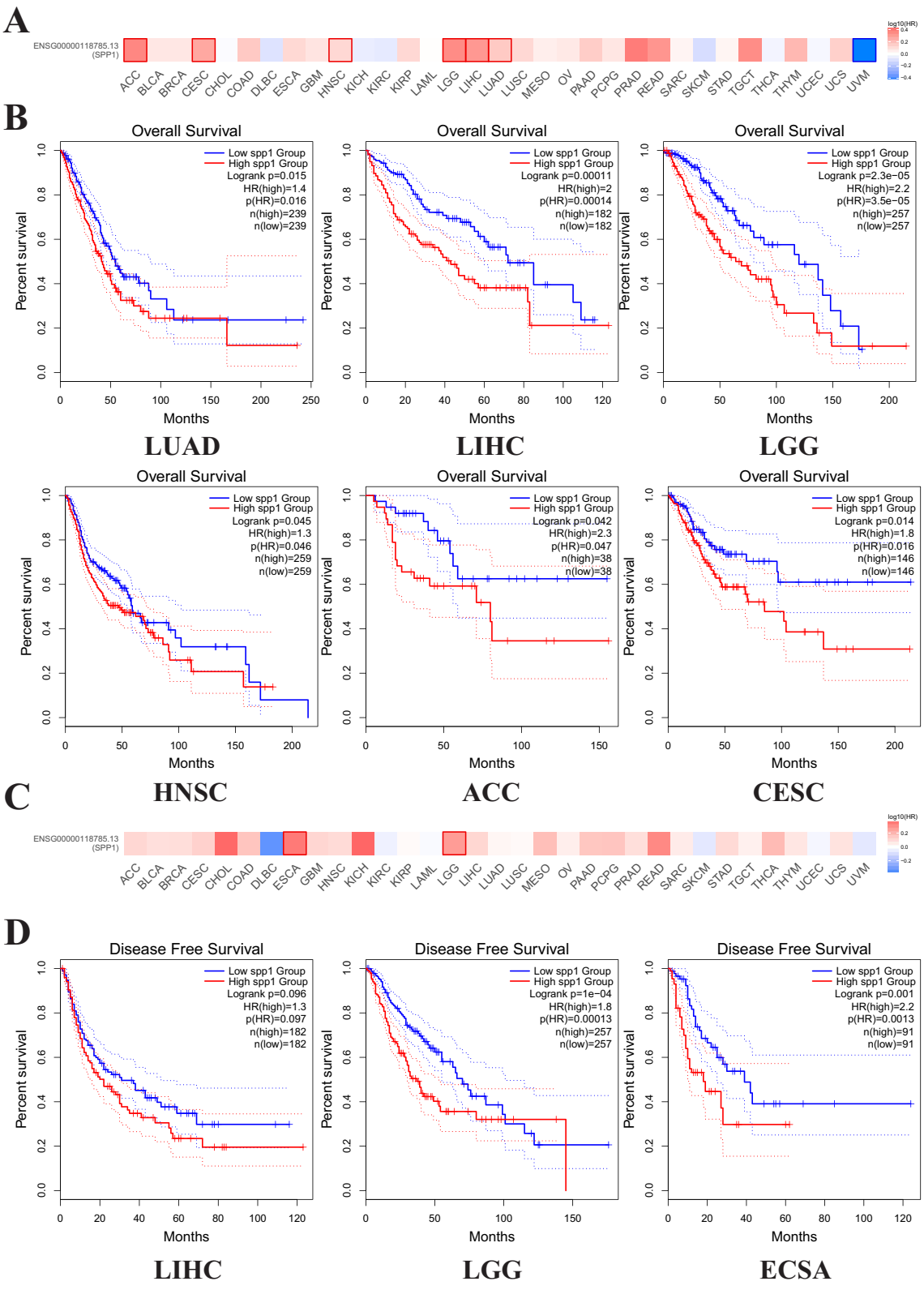

Figure 2 Correlation of *SPP1* Expression with Survival Outcomes in Various Cancers. (**A**) Correlation between *SPP1* and OS in various cancers. (**B**) Patients with low *SPP1* expression have higher overall survival rates in LUAD, LIHC, LGG, HNSC, ACC, and CESC compared to high *SPP1* expression patients. (**C**) Correlation between *SPP1* and DFS in various cancers. (**D**) High *SPP1* expression is associated with shorter DFS in LIHC, LGG, and ECSA.

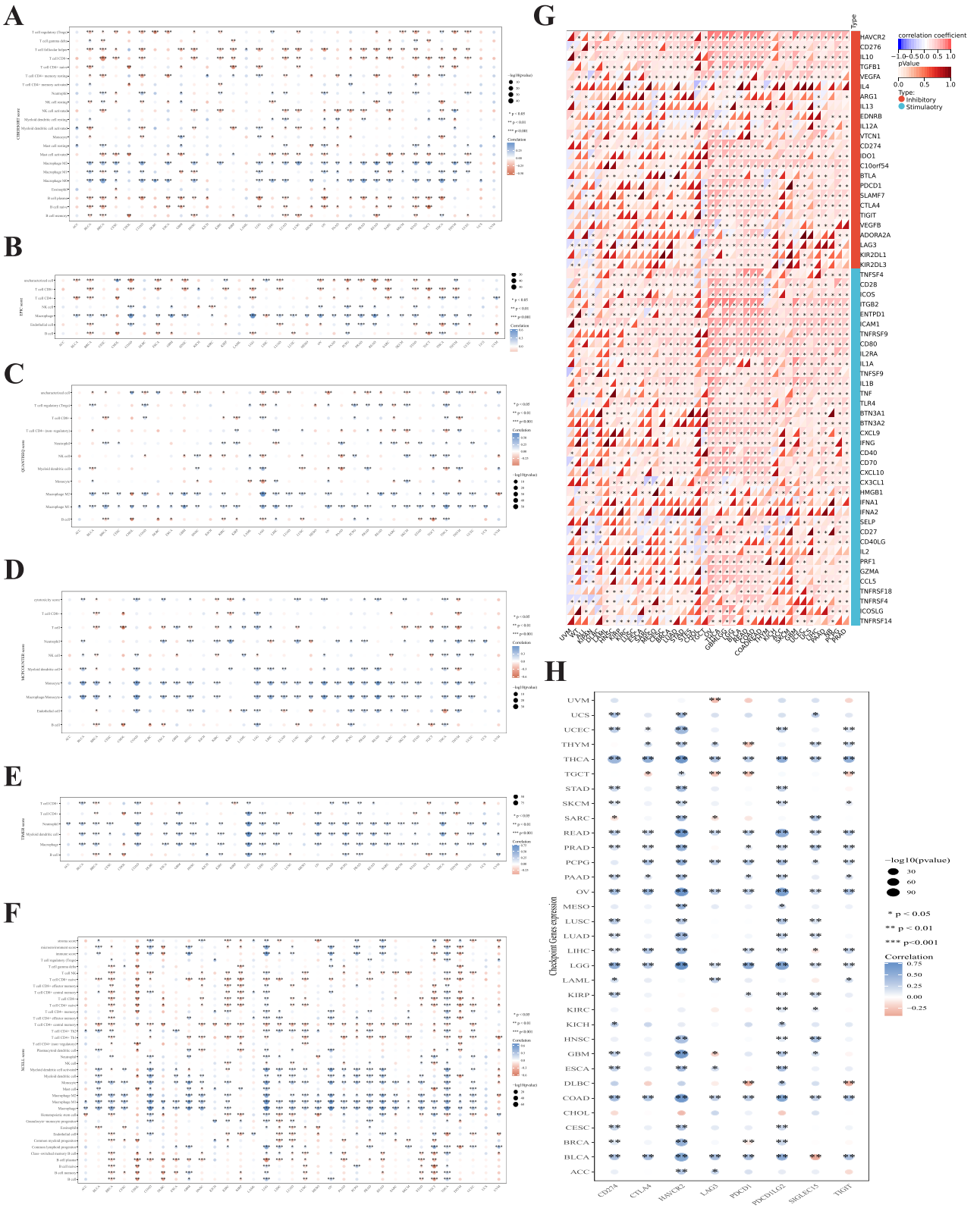

Figure 3 Continued.

https://doi.org/10.2147/JIR.S505237

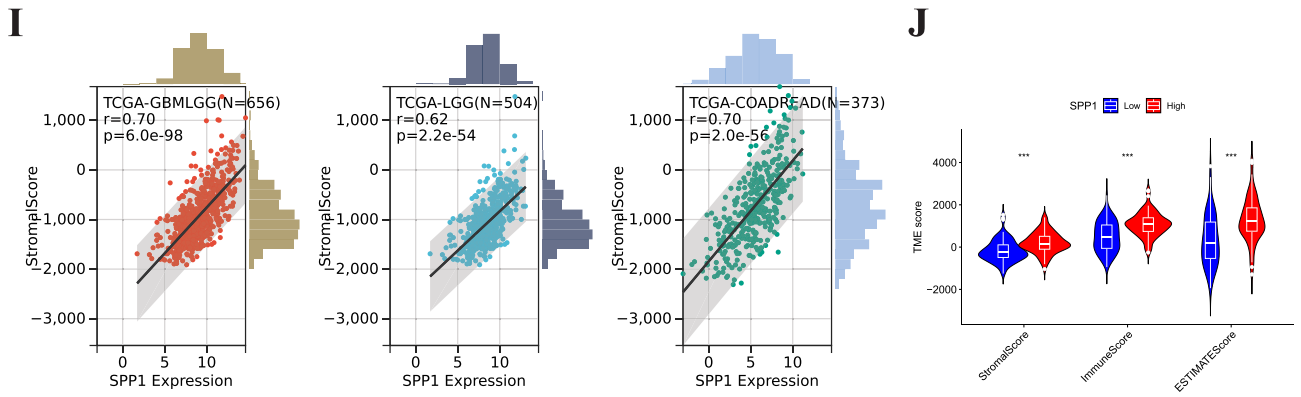

Figure 3 Association of *SPP1* with Immune Cells and Pathways in Cancers. (**A**–**F**) Immune cell analysis using CIBERSORT, EPIC, QUANTISEQ, MCPcounter, TIMER, and XCELL showing the association of *SPP1* with different immune cells in cancers. (**G** and **H**) Correlation of *SPP1* with marker genes of immune pathways in different tumors. (**I**) Correlation between *SPP1* expression levels and StromalScore in GBM and LGG. (**J**) *SPP1* expression levels positively correlate with TME (Tumor Microenvironment) scores. *p < 0.05, **p < 0.01, ***p < 0.001.

The Relationship Between SPP1, RNA Gene Modifications, Gene Mutations, and Tumor Stemness Index

Tumor Mutation Burden (TMB) Indicates the Number of Mutations Within a Tumor Sample. Correlation analysis was used to explore the relationship between SPP1 and TMB across different tumors. Statistical significance was set at $P < 0.05$. The results showed that DLBC, UCS, COAD, and STAD were significantly positively correlated with SPP1, while CHOL, UVM, KIRC, and LUSC were significantly negatively correlated with SPP1 (Figure S3A). However, the results were inconsistent in GBM and LGG (Figure S3B and C). In GBM, the SPP1 gene shows significant positive and negative correlations with several RNA modification genes, such as YTHDF1, NSUN2, TRMT6, and DNMT1. These correlations are statistically significant, suggesting that these RNA modification genes may play crucial roles in the development of GBM (Figure S3D). Microsatellite Instability (MSI) is an important tumor marker associated with mutations. The correlation results showed that SPP1 was significantly positively correlated with MSI in COAD, STAD, and TGCT, and significantly negatively correlated with MSI in GBM, LGG, KICH, HNSC, and UVM (Figure S3E). Tumor stemness refers to the critical role of cancer stem cells in tumor initiation, progression, and recurrence. The RNAss analysis showed that we observed significant correlations in 37 tumors, with 7 tumors showing a significant positive correlation and 30 tumors showing a significant negative correlation. Among them, SPP1 was negatively correlated with tumor stemness in gliomas (Figure S3F).

SPP1 Gene Association and Enrichment Analysis

To better understand the molecular mechanisms of SPP1 in tumorigenesis and development, this study downloaded the top 100 genes significantly associated with SPP1 from the GEPIA online database. Subsequently, the STRING tool was used to construct an interaction molecular network, identifying 24 experimentally validated SPP1-binding molecules (Figure 4A). Additionally, we explored their potential functions.

KEGG analysis results showed that SPP1-related molecules are associated with cell adhesion molecules and lysosomes (Figure 4B). GO enrichment results indicated that SPP1-related molecules are significantly associated with the Notch signaling pathway and regulation of leukocyte activation (Figure 4C). Finally, to further explore the molecular mechanisms of SPP1 in the occurrence and development of GBM, the gene-pathway correlation analysis showed that in GBM patients, SPP1 might participate in the occurrence and development of GBM by regulating the following signaling pathways: Tumor Inflammation Signature, Cellular response to hypoxia, Tumor proliferation signature, EMT markers, ECM-related genes, Angiogenesis, Apoptosis, DNA repair, and G2M_checkpoint (Figure 4D).

Single-Cell Analysis of SPP1 Expression in GBM Patients

Given the prognostic value and abnormal distribution of SPP1 in GBM tissues, we aimed to identify the specific cell types enriched with SPP1 using scRNA-seq. Analysis of the GSE131928 dataset revealed 26 distinct cell clusters (Figure 5A) and 8 major cell types (Figure 5B) within GBM tissues. The marker genes for each cell type are presented in figure, where we also quantified the proportion of each cell type and detailed the infiltration levels in each sample (Figure 5C and D).

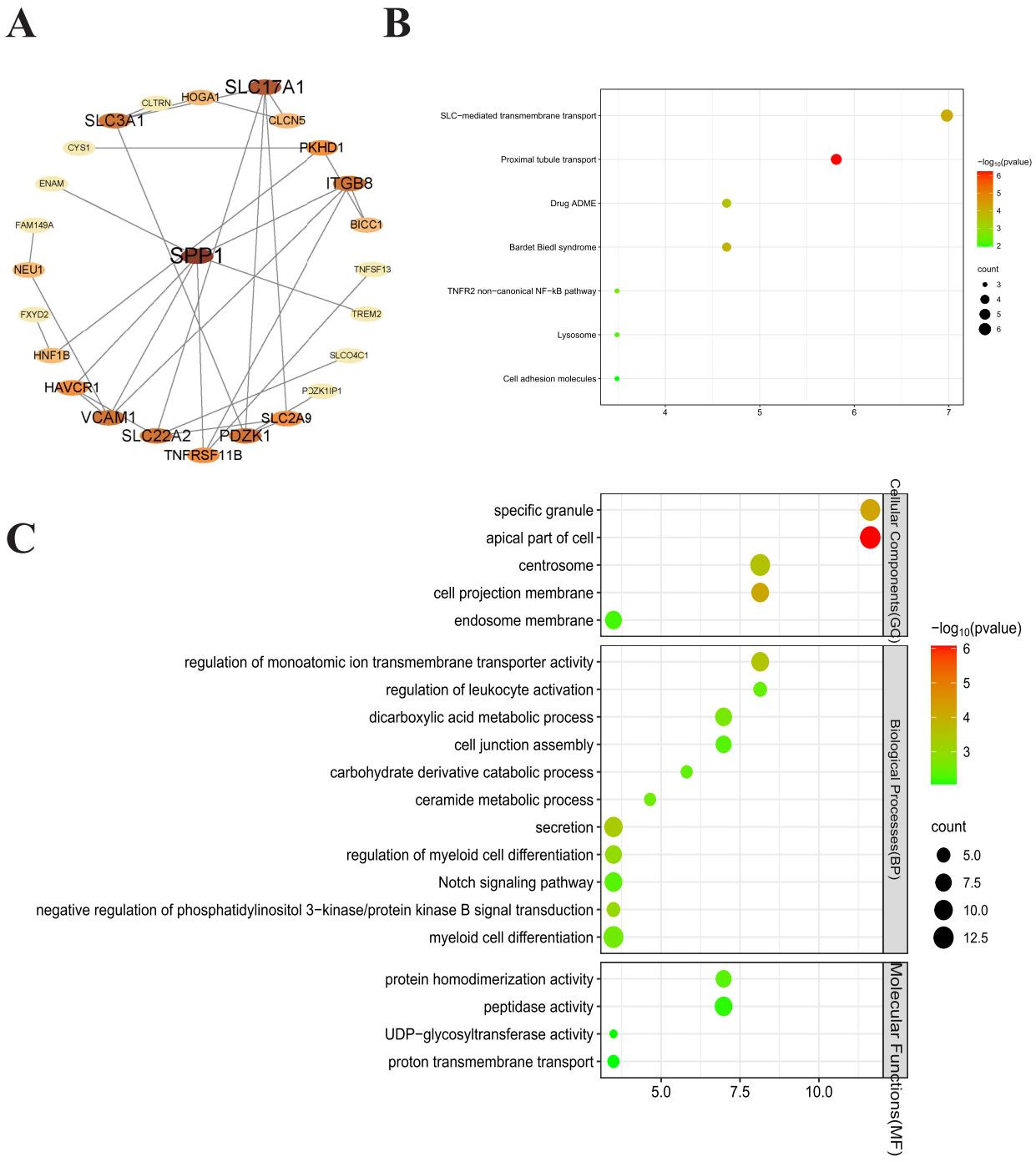

Figure 4 Continued.

https://doi.org/10.2147/JIR.S505237

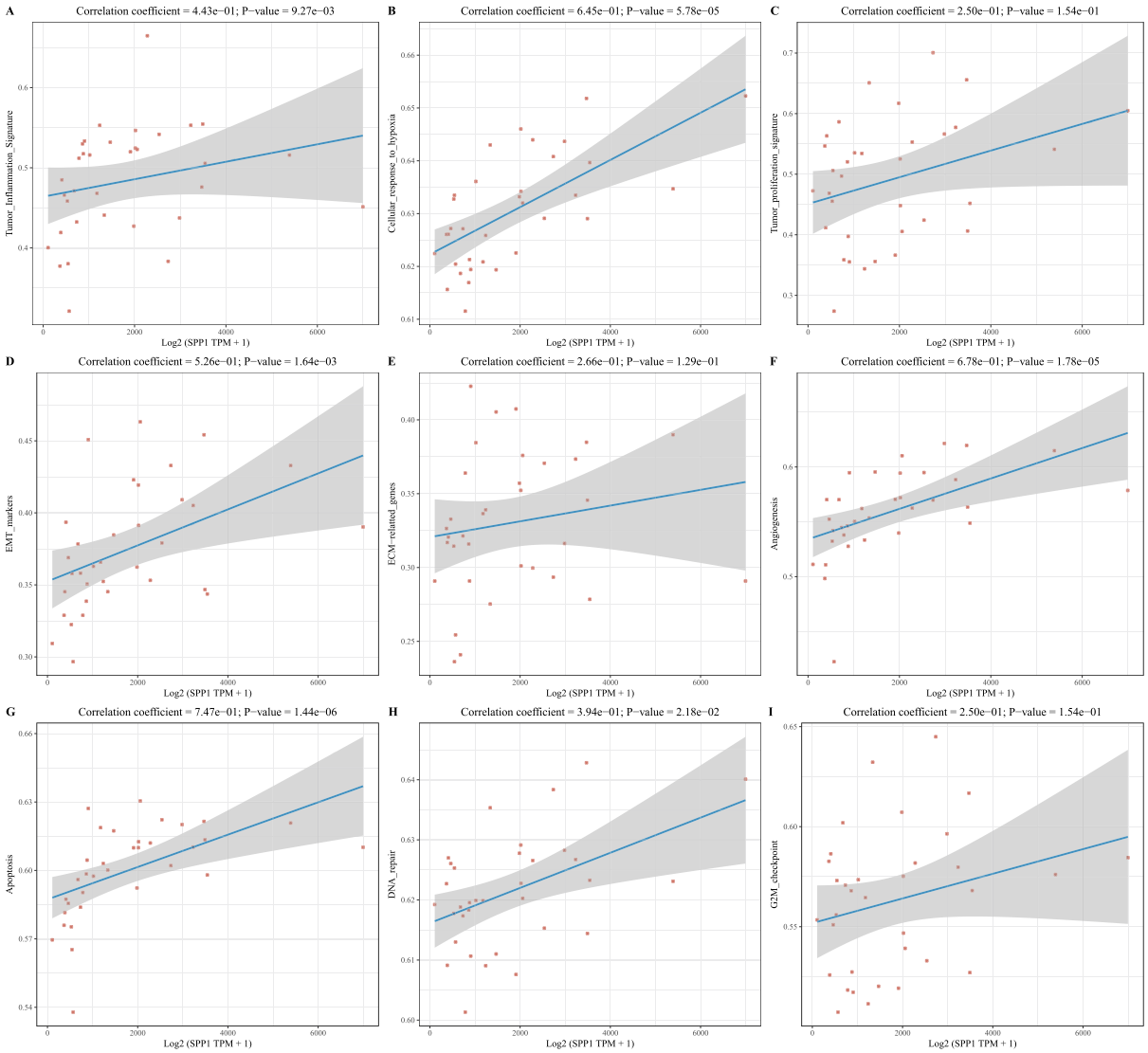

Figure 4 Molecular Network and Pathway Analysis of Genes Associated with *SPP1*. (**A**) Network relationship of the top 30 genes significantly associated with *SPP1*. (**B**) KEGG analysis shows *SPP1*-associated molecules are related to cell adhesion molecules and lysosomes. (**C**) GO analysis indicates *SPP1*-associated molecules are significantly related to the Notch signaling pathway. (**D**) [a-l] Gene-pathway correlation analysis shows *SPP1* is closely related to Apoptosis, DNA repair, and G2M checkpoint.

UMAP visualizations of SPP1 expression in glioma cells were generated (Figure 5E). Cell-cell interaction analysis indicated that SPP1-positive macrophages primarily interact with malignant GBM cells and T cells (Figure 5F). Additionally, our findings revealed that SPP1 is significantly enriched in monocytes/macrophages (Figure 5G).

Analysis of SPP1 Expression and Drug Sensitivity in GBM Patients

To further investigate drugs sensitive to SPP1, we explored the chemotherapy drug sensitivity predicted by genomic data. Chemotherapy drugs were screened using clinical trials and FDA approval as thresholds, and the Pearson correlation coefficient between the predicted genome and chemotherapy drugs was calculated. Significant drugs were visualized and ranked according to p-value. Our results indicate that SPP1 is significantly correlated with CUDC-101, GSK690693, Imatinib, LAQ824, and OSI-027 (Figure 6A–E).

Aberrant Overexpression of SPP1 in GBM

To further investigate the impact of SPP1 on gliomas, we initially conducted differential expression analysis using the TCGA-GBM dataset, TCGA-LGG dataset, and the Genotype-Tissue Expression (GTEx) database. The results revealed that SPP1 expression was significantly increased in glioma samples (GBM and LGG) compared to normal tissues ($P < 0.001$; Figure 6F). Previous pan-cancer data also indicated that SPP1 expression is significantly correlated with tumor grade in glioma patients. Additionally, by comparing normal astrocytes and glioma cell lines, we validated the overexpression of SPP1 in GBM cell lines through PCR and Western Blot (Figure 6G and H).

Knockdown of SPP1 Inhibits Malignant Progression of Glioma Cell Lines

To verify the function of SPP1 in gliomas, we knocked down SPP1 expression in various glioma cell lines using siRNA-mediated methods (Figure 6I and J). The results showed that knockdown of SPP1 significantly inhibited the proliferation and invasion abilities of glioma cells (Figure 7A, B, D and F). Additionally, flow cytometry analysis indicated that SPP1

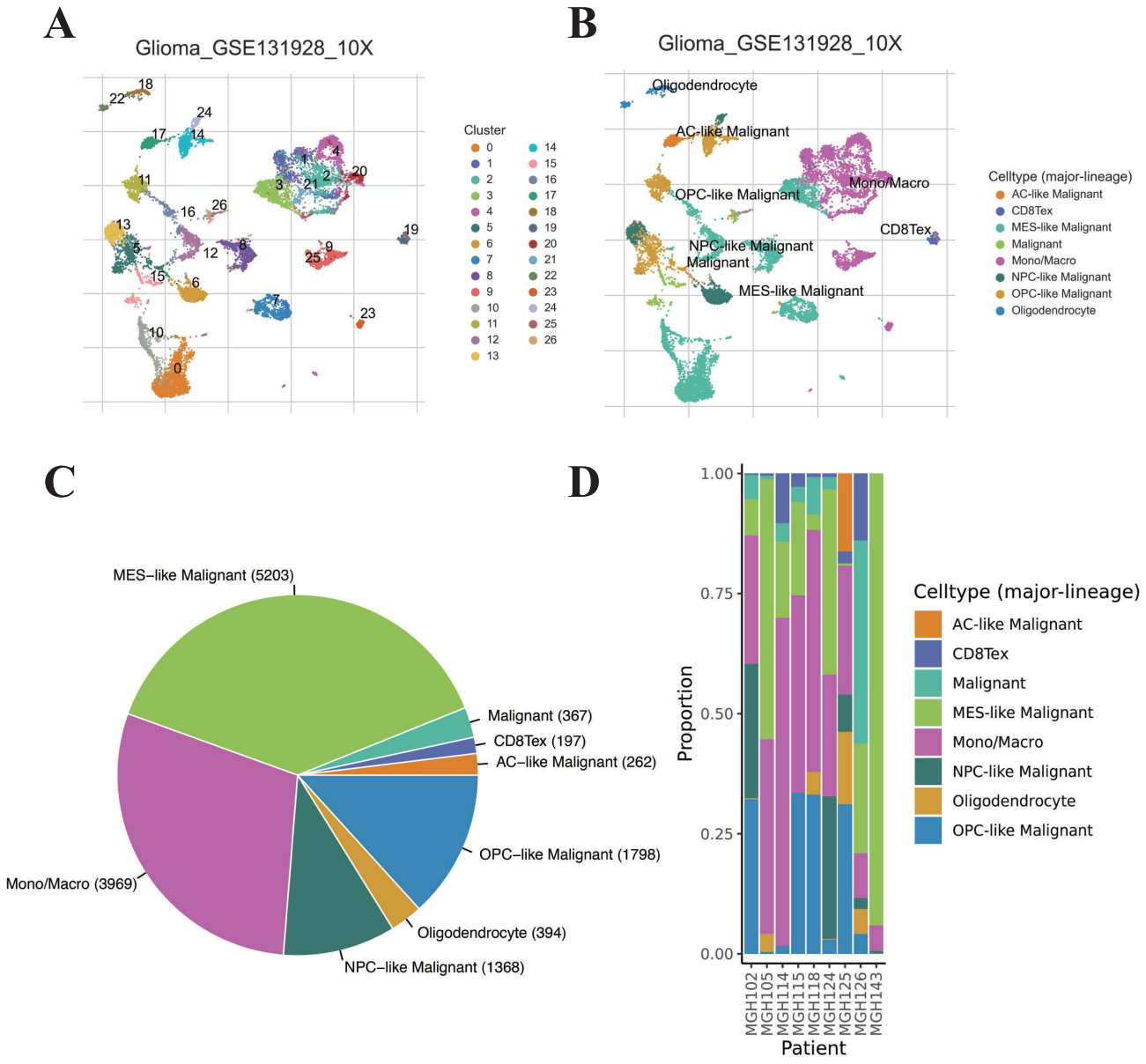

Figure 5 Continued.

https://doi.org/10.2147/JIR.S505237

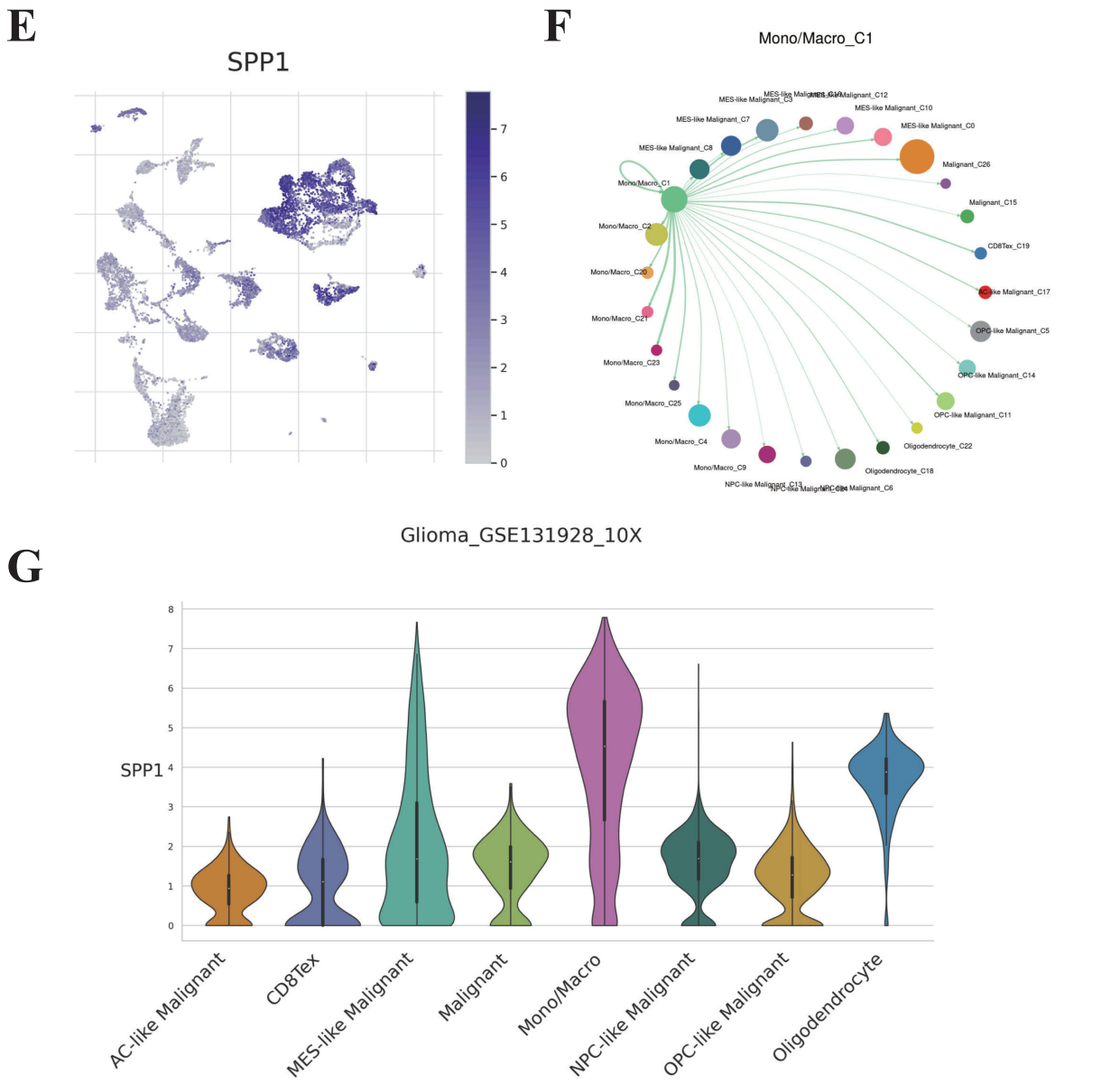

Figure 5 Single-Cell Analysis of *SPP1* Expression and Cell Type Distribution in GBM. (**A** and **B**) 26 cell clusters and 8 cell types were identified in GBM tissues using scRNA-seq. (**C** and **D**) Proportions of each cell type in scRNA-seq of GBM and detailed infiltration of each cell type in each sample. (**E**) UMAP visualization of *SPP1* expression in glioma cells. (**F**) CCI analysis shows *SPP1* macrophages primarily interact with malignant GBM cells and T cells. (**G**) *SPP1* is significantly enriched in monocytes/macrophages in GBM.

knockdown caused cell cycle arrest in the G0/G1 phase and promoted apoptosis, suggesting that SPP1 plays an important role in regulating the cell cycle and apoptosis in glioma cells (Figure 7C and E). Overall, these findings suggest that SPP1 promotes the malignant progression of glioma cells, and its inhibition may serve as a new strategy for glioma therapy.

Discussion

The results of our pan-cancer analysis underscore the significant role of *SPP1* as a prognostic and immunotherapeutic biomarker across various cancer types, including gliomas. The overexpression of *SPP1* in 27 out of 33 tumor types, such as GBM and LGG, highlights its pervasive involvement in cancer biology. This discussion will focus on the implications of these findings for cancer prognosis, tumor microenvironment interactions, and potential therapeutic strategies.

Our study demonstrates that high *SPP1* expression is consistently associated with poor OS, PFS, DFS, and DSS across multiple cancer types. Specifically, in GBM and LGG, elevated *SPP1* levels correlate with significantly reduced survival times. These findings align with previous studies indicating *SPP1*'s role in promoting tumor aggressiveness and poor clinical outcomes.[12,13] The consistent correlation between *SPP1* expression and adverse prognostic indicators underscores its potential as a robust biomarker for predicting patient outcomes and stratifying patients based on risk.[6,14,15]

SPP1's overexpression is significantly associated with immune cell infiltration, particularly $CD8^+$ T cells and macrophages, across various cancers.[16–18] In GBM, single-cell analysis reveals that *SPP1* is enriched in macrophages and interacts with malignant cells, suggesting its role in modulating the tumor microenvironment. The strong correlation between *SPP1* expression and immune checkpoint-related genes further indicates its involvement in immune evasion

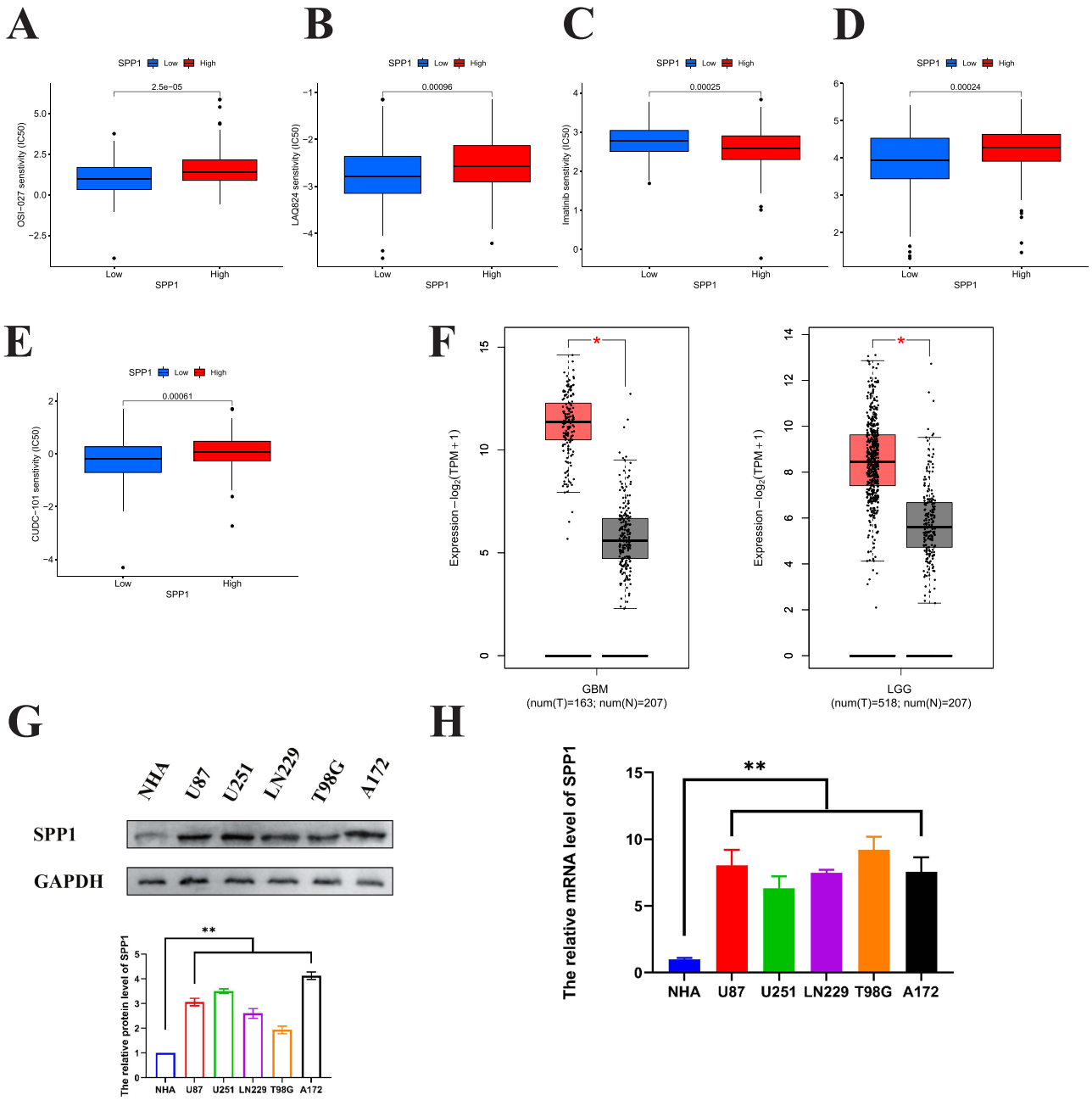

Figure 6 Continued.

https://doi.org/10.2147/JIR.S505237

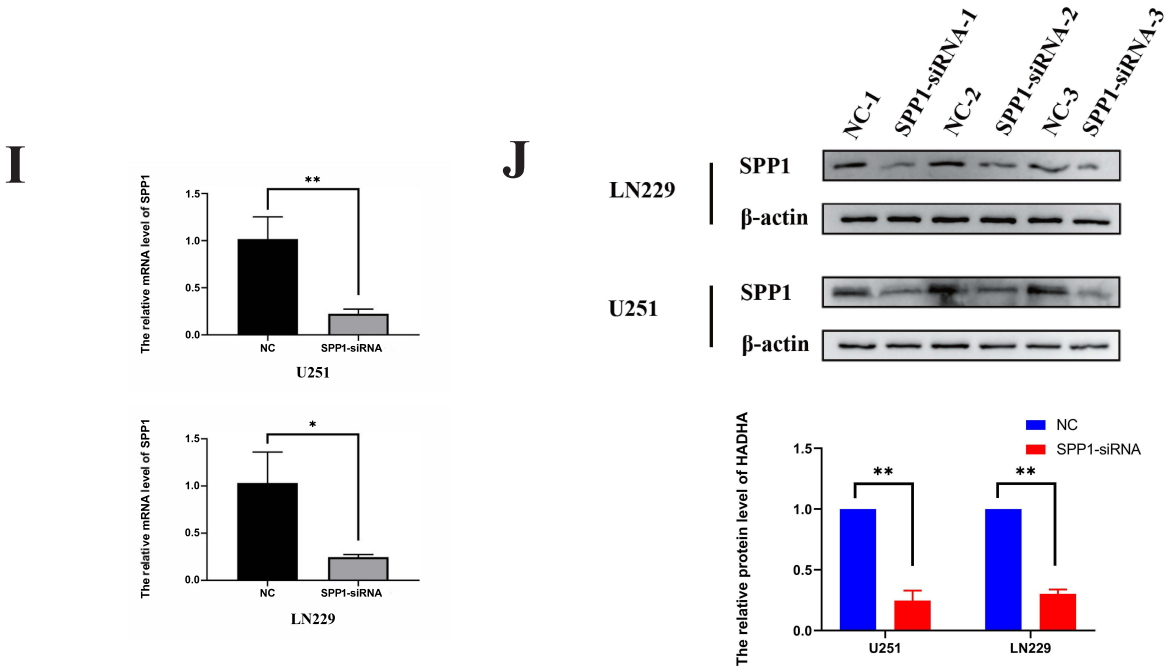

Figure 6 Impact of *SPP1* on Drug Sensitivity, Expression in GBM. (**A**–**E**) *SPP1* and drug sensitivity analysis. (**F**) Differential analysis shows *SPP1* expression is significantly higher in GBM and LGG compared to normal tissues. (**G** and **H**) WB and PCR results show *SPP1* expression is significantly higher in glioma cell lines compared to NHA. (**I** and **J**) WB and PCR analysis of *SPP1*-siRNA knockdown efficiency. *p < 0.05, **p < 0.01.

mechanisms.[19] These interactions suggest that *SPP1* not only contributes to tumor progression but also plays a pivotal role in shaping the immune landscape within tumors.

Given *SPP1*'s significant overexpression and its association with poor prognosis and immune modulation, targeting *SPP1* presents a novel therapeutic strategy. Knockdown experiments in glioma cell lines demonstrated that reducing *SPP1* expression inhibits cell proliferation, migration, and invasion. These results indicate that *SPP1* is a viable target for therapeutic intervention, particularly in tumors where current immunotherapies have shown limited efficacy, such as GBM. Our findings align with Pang et al, who demonstrated that *SPP1* promotes enzalutamide resistance and in castration-resistant prostate cancer (CRPC) by activating the PI3K/AKT and ERK1/2 pathways. They found that knocking down *SPP1* enhances enzalutamide sensitivity and inhibits CRPC cell invasion and migration, highlighting the therapeutic potential of targeting *SPP1* in resistant prostate cancer.[20] Developing therapies that target *SPP1* could enhance the effectiveness of existing treatments and improve patient outcomes.

While our study provides compelling evidence for *SPP1* as a prognostic and immunotherapeutic biomarker, further research is needed to validate these findings in clinical settings. Future studies should focus on elucidating the specific mechanisms of action of SPP1 in brain tumors, including its molecular pathways and regulatory mechanisms in tumor cell proliferation, invasion, and immune evasion. Future studies should focus on elucidating the specific mechanisms of action of SPP1 in brain tumors, including its molecular pathways and regulatory mechanisms in tumor cell proliferation, invasion, and immune evasion. This will help develop more precise targeted therapeutic strategies, enhancing the efficacy and specificity of SPP1-targeted therapies.

Additionally, conducting in vivo experiments is an essential direction for future research. Validating the effects and safety of SPP1-targeted therapies in animal models can provide a more reliable basis for clinical trials. For example, using glioblastoma mouse models to assess the impact of SPP1 inhibitors on tumor growth, metastasis, and animal survival, while monitoring potential toxic side effects, can optimize treatment protocols and dosages.

We should also pay attention to the combination of SPP1-targeted therapies with other treatment modalities. Exploring the synergistic effects of SPP1 inhibition with immune checkpoint inhibitors, radiotherapy, and chemotherapy may yield better treatment outcomes. For instance, SPP1 inhibitors may enhance the blockade of tumor immune evasion by immune checkpoint inhibitors, or when combined with radiotherapy and chemotherapy, increase the sensitivity of tumor cells to treatment, achieving a multi-pathway, multi-level anti-tumor effect.[21,22]

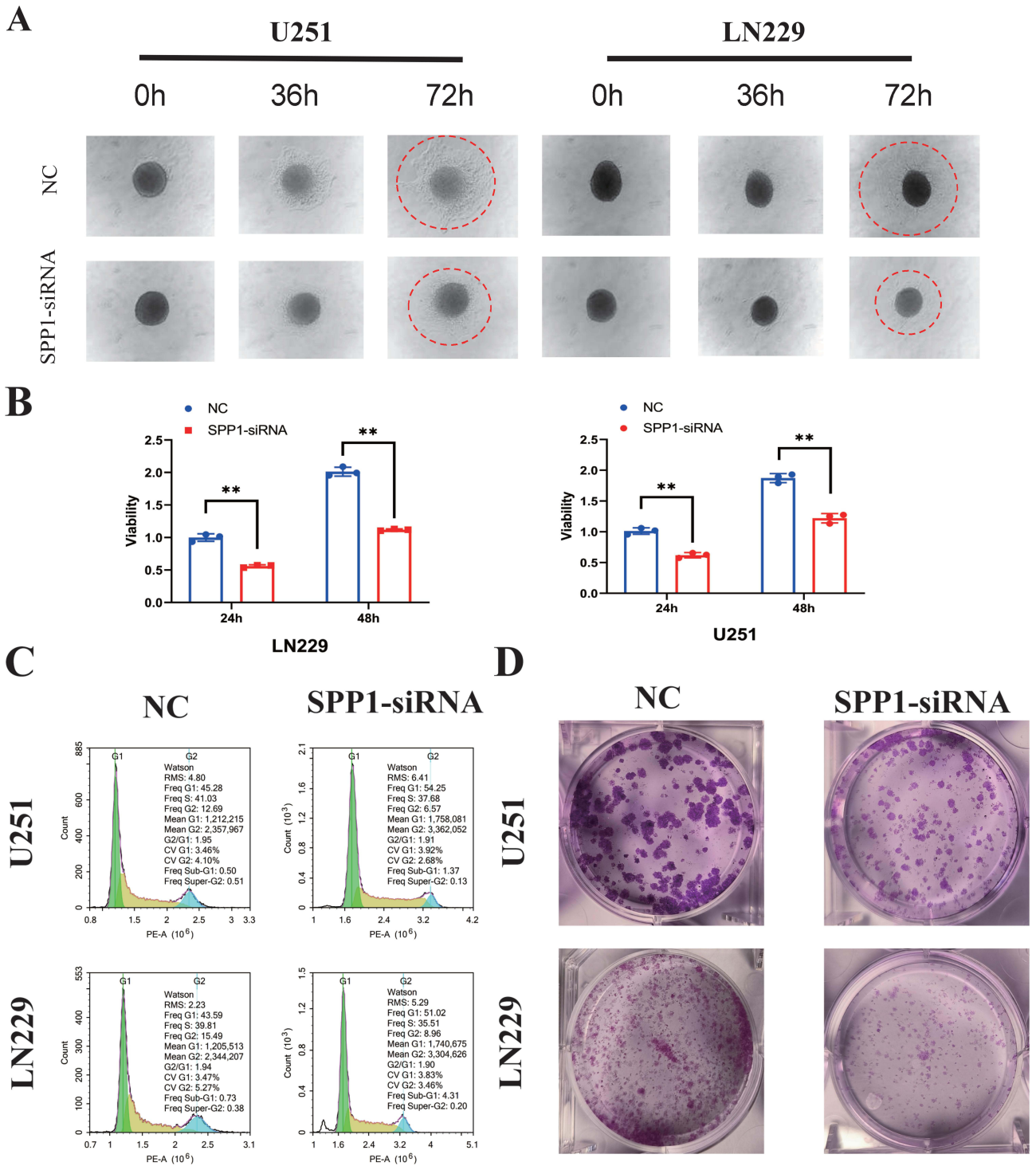

Figure 7 Continued.

https://doi.org/10.2147/JIR.S505237

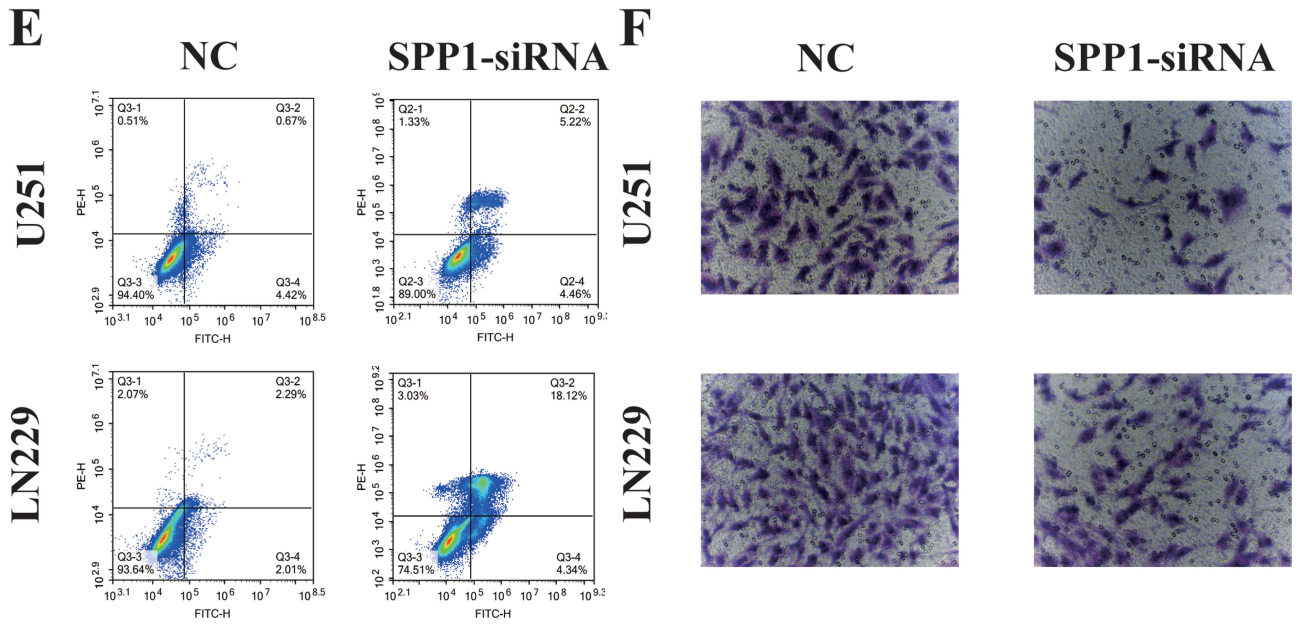

Figure 7 Knockdown of *SPP1* inhibits the malignant progression of glioma cells. (**A**) Knockdown of *SPP1* inhibits the invasive properties of glioma cells in a three-dimensional environment. (**B**) CCK8 assay shows that *SPP1* knockdown significantly inhibits glioma cell proliferation. (**C**) Cell cycle analysis shows *SPP1* knockdown leads to cell cycle arrest at the G0/G1 phase. (**D**) Knockdown of *SPP1* reduces colony formation in glioma cells. (**E**) Knockdown of *SPP1* promotes apoptosis in glioma cells. (**F**) Transwell assay shows *SPP1* knockdown significantly inhibits glioma cell invasion. **p < 0.01.

Conclusion

In conclusion, our comprehensive pan-cancer analysis highlights SPP1's potential as a prognostic and immunotherapeutic biomarker in various cancers, including gliomas. Its overexpression correlates with poor prognosis and significant immune cell infiltration, suggesting that targeting SPP1 could be a promising strategy for improving cancer treatment outcomes. Further research and clinical validation are necessary to fully harness SPP1's potential in cancer therapy.

Research Ethics and Consent

We utilize publicly available data obtained through legal means, which complies with Article 32, Item 1 of the "Ethical Review Measures for Life Sciences and Medical Research Involving Human Subjects". This research does not cause harm to individuals, does not involve sensitive personal information, or commercial interests, and thus can be exempted from ethical review.

Acknowledgments

We would like to thank all the patients enrolled in this study.

Author Contributions

All authors made a significant contribution to the work reported, whether that is in the conception, study design, execution, acquisition of data, analysis and interpretation, or in all these areas; took part in drafting, revising or critically reviewing the article; gave final approval of the version to be published; have agreed on the journal to which the article has been submitted; and agree to be accountable for all aspects of the work.

Funding

This research received no external funding.

Disclosure

The author(s) report no conflicts of interest in this work.

References

1. Siegel RL, Giaquinto AN, Jemal A. Cancer statistics, 2024. *CA Cancer J Clin*. 2024;74(1):12–49. doi:10.3322/caac.21820
2. Ostrom QT, Price M, Neff C, et al. CBTRUS Statistical Report: primary Brain and Other Central Nervous System Tumors Diagnosed in the United States in 2016–2020. *Neuro Oncol*. 2023;25(12 Suppl 2):iv1–iv99. doi:10.1093/neuonc/noad149
3. Lim M, Xia Y, Bettegowda C, Weller M. Current state of immunotherapy for glioblastoma. *Nat Rev Clin Oncol*. 2018;15(7):422–442. doi:10.1038/s41571-018-0003-5
4. Rong L, Li N, Zhang Z. Emerging therapies for glioblastoma: current state and future directions. *J Exp Clin Cancer Res*. 2022;41(1):142. doi:10.1186/s13046-022-02349-7
5. Zhao H, Chen Q, Alam A, et al. The role of osteopontin in the progression of solid organ tumour. *Cell Death Dis*. 2018;9(3):356. doi:10.1038/s41419-018-0391-6
6. Yu S, Chen M, Xu L, Mao E, Sun S. A senescence-based prognostic gene signature for colorectal cancer and identification of the role of SPP1-positive macrophages in tumor senescence. *Front Immunol*. 2023;14:1175490. doi:10.3389/fimmu.2023.1175490
7. Wei R, Wong JPC, Kwok HF. Osteopontin – a promising biomarker for cancer therapy. *J Cancer*. 2017;8(12):2173–2183. doi:10.7150/jca.20480
8. Lamour V, Henry A, Kroonen J, et al. Targeting osteopontin suppresses glioblastoma stem-like cell character and tumorigenicity in vivo. *Int J Cancer*. 2015;137(5):1047–1057. doi:10.1002/ijc.29454
9. Malta TM, Sokolov A, Gentles AJ, et al. Machine Learning Identifies Stemness Features Associated with Oncogenic Dedifferentiation. *Cell*. 2018;173(2):338–354.e15. doi:10.1016/j.cell.2018.03.034
10. Wei J, Huang K, Chen Z, et al. Characterization of Glycolysis-Associated Molecules in the Tumor Microenvironment Revealed by Pan-Cancer Tissues and Lung Cancer Single Cell Data. *Cancers*. 2020;12(7):1788. doi:10.3390/cancers12071788
11. Neftel C, Laffy J, Filbin MG, et al. An Integrative Model of Cellular States, Plasticity, and Genetics for Glioblastoma. *Cell*. 2019;178(4):835–849.e21. doi:10.1016/j.cell.2019.06.024
12. Zou Y, Tan X, Yuan G, et al. SPP1 is associated with adverse prognosis and predicts immunotherapy efficacy in penile cancer. *Hum Genomics*. 2023;17(1):116. doi:10.1186/s40246-023-00558-5
13. Bie T, Zhang X. Higher Expression of SPP1 Predicts Poorer Survival Outcomes in Head and Neck Cancer. *J Immunol Res*. 2021;2021:8569575. doi:10.1155/2021/8569575
14. Annadurai Y, Easwaran M, Sundar S, et al. SPP1, a potential therapeutic target and biomarker for lung cancer: functional insights through computational studies. *J Biomol Struct Dyn*. 2024;42(3):1336–1351. doi:10.1080/07391102.2023.2199871
15. Wu Y, Ren L, Tang Y, et al. Immunobiological signatures and the emerging role of SPP1 in predicting tumor heterogeneity, malignancy, and clinical outcomes in stomach adenocarcinoma. *Aging*. 2023;15(20):11588–11610. doi:10.18632/aging.205148
16. Wang K, Hou H, Zhang Y, Ao M, Luo H, Li B. Ovarian cancer-associated immune exhaustion involves SPP1+ T cell and NKT cell, symbolizing more malignant progression. *Front Endocrinol*. 2023;14:1168245. doi:10.3389/fendo.2023.1168245
17. Liu L, Zhang R, Deng J, et al. Construction of TME and Identification of crosstalk between malignant cells and macrophages by SPP1 in hepatocellular carcinoma. *Cancer Immunol Immunother*. 2022;71(1):121–136. doi:10.1007/s00262-021-02967-8
18. Su X, Liang C, Chen R, Duan S. Deciphering tumor microenvironment: CXCL9 and SPP1 as crucial determinants of tumor-associated macrophage polarity and prognostic indicators. *mol Cancer*. 2024;23(1):13. doi:10.1186/s12943-023-01931-7
19. Xiang T, Cheng N, Huang B, Zhang X, Zeng P. Important oncogenic and immunogenic roles of SPP1 and CSF1 in hepatocellular carcinoma. *Med Oncol*. 2023;40(6):158. doi:10.1007/s12032-023-02024-7
20. Pang X, Zhang J, He X, et al. SPP1 Promotes Enzalutamide Resistance and Epithelial-Mesenchymal-Transition Activation in Castration-Resistant Prostate Cancer via PI3K/AKT and ERK1/2 Pathways. *Oxid Med Cell Longev*. 2021;2021(1):5806602. doi:10.1155/2021/5806602
21. Wang C, Li Y, Wang L, et al. SPP1 represents a therapeutic target that promotes the progression of oesophageal squamous cell carcinoma by driving M2 macrophage infiltration. *Br J Cancer*. 2024;130(11):1770–1782. doi:10.1038/s41416-024-02683-x
22. Chen X, Xiong D, Ye L, et al. SPP1 inhibition improves the cisplatin chemo-sensitivity of cervical cancer cell lines. *Cancer Chemother Pharmacol*. 2019;83(4):603–613. doi:10.1007/s00280-018-3759-5